AIMS Mathematics, 9(8): 20742–20762.
DOI:10.3934/math.20241008
Received: 23 April 2024
Revised: 02 June 2024
Accepted: 12 June 2024
Published: 26 June 2024

http://www.aimspress.com/journal/Math

Research article

Echo state network-based adaptive control for nonstrict-feedback nonlinear systems with input dead-zone and external disturbance

Hadil Alhazmi[1] **and Mohamed Kharrat**[2,*]

[1] Department of Mathematical Sciences, College of Science, Princess Nourah Bint Abdulrahman University, P.O. Box 84428, Riyadh 11671, Saudi Arabia

[2] Department of Mathematics, College of Science, Jouf University, P.O. Box 2014, Sakaka, Saudi Arabia

* **Correspondence:** Email: mkharrat@ju.edu.sa.

Abstract: This paper addressed the adaptive control problem for non-strict-feedback nonlinear systems with dead-zone and external disturbances. The design methodology integrated the backstepping technique with the approximation of unknown functions using an echo state network (ESN), enabling real-time adjustments. A comprehensive Lyapunov stability study was conducted to confirm the semi-globally uniformly ultimately boundedness (SGUUB) of all signals in the closed-loop system, ensuring that the tracking error converged to a small neighborhood of the origin. The effectiveness of the proposed method was further demonstrated through two examples, and error assessment criteria were utilized for comparisons with existing controllers.

Keywords: adaptive control; Lyapunov function; nonlinear systems; dead-zone; external disturbance; echo state network; error assessment criteria
Mathematics Subject Classification: 92B20, 93C10, 93C40

1. Introduction

In recent years, there has been a growing interest in addressing the nonlinear aspects inherent in practical physical systems [1–5]. Consequently, there is an increasing demand for control approaches capable of effectively managing complex nonlinear systems. Various control methods have been developed to tackle tracking or stabilization control objectives. One widely adopted approach is the adaptive backstepping technique, recognized as a recursive design procedure suitable for controller design in nonlinear dynamic systems. To address the output maneuvering control problem in nonlinear systems, a study was conducted using the backstepping technique [6–8]. An adaptive robust backstepping approach was proposed to attain a specified performance level for these nonlinear

systems. It is important to note that this approach assumes knowledge or linear parameterization of the structural uncertainties present in the nonlinear systems [9, 10].

In various practical engineering applications, uncertainties arise not only from nonlinearities but also from parameter variations, contributing to uncertain functions within the systems [11]. This complexity hinders the direct application of simple adaptive backstepping control techniques. Researchers have responded by integrating the adaptive backstepping control framework with the approximation capabilities of neural networks (NNs) and fuzzy logic systems (FLSs) to address this challenge [12]. For nonlinear systems under feature information, the adaptive control problem has been reported via prescribed performance [13]. For strict-feedback nonlinear systems, an adaptive control method has been published via event-triggered mechanism [14] For strict-feedback nonlinear systems, an adaptive fuzzy control problem has been published under the impact of control gain unknown functions [15]. For high-order nonlinear systems, a multilayer neuro control problem has been reported under the impact of active disturbance rejection [16]. For nonlinear mismatched systems, a new integral robust method based on asymptotic tracking has been published [17].

Through the incorporation of these techniques, adaptive neural or fuzzy backstepping control strategies have been developed, effectively tackling control issues in nonlinear systems characterized by both uncertain parameters and uncertain functions. These advanced strategies enable the successful management of uncertainties in real-world systems, enhancing their overall control performance.

At this point, radial basis function neural networks (RBFNNs) were employed to tackle time-varying uncertainty. As an alternative approximation technique, RBFNNs were static feed-forward networks with a substantial number of neurons, enhancing the accuracy of the approximation. The authors in [18] introduced recurrent neural networks (RNNs) with dynamic feedback structures to model dynamic systems. In addressing the issue of time consumption, echo state network (ESN) was introduced, offering an alternative approach to train RNNs [19]. ESN has recently demonstrated its efficacy in improving the approximation performance of uncertain nonlinearities across various nonlinear systems. From the literature, it becomes evident that ESN proves advantageous in effectively approximating unknown functions [20].

It is widely recognized that non-strict-feedback nonlinear systems encompass a broader range of system forms compared to systems with strict-feedback nature [21]. In real-world applications, various types of nonlinear systems, including the ball and beam system [22, 23], often exhibit non-strict-feedback structures. A notable characteristic of non-strict-feedback systems is their dependence on all system states when defining the system functions. This poses significant difficulties and challenges when designing control schemes using the backstepping technique [24]. Consequently, addressing control design for non-strict-feedback systems is an intriguing and valuable topic, both in theoretical research and practical applications, with numerous results documented [25–27]. For instance, for non-strict-feedback nonlinear systems, an adaptive control method based on fuzzy approximation has been published under function constraints [28]. Additionally, a fuzzy adaptive asymptotic method for non-strict-feedback nonlinear systems has been reported [29].

In the field of control engineering, non-smooth nonlinearities such as backlash, hysteresis, and dead-zones are commonly observed between actuators and sensors [30]. Dead-zones, being non-smooth functions, can significantly degrade system performance and even lead to instability [31]. Therefore, it is necessary to consider the presence of dead-zones during the controller design process. In recent years, several research studies have addressed the challenges posed by dead-zones in nonlinear

systems [32]. For example, a novel adaptive robust backstepping control scheme has been proposed to tackle the dead-zone problem in nonlinear dynamic systems [12]. Additionally, an adaptive neural controller utilizing a combination of dynamic surface control (DSC) and neural networks (NNs) has been developed for a specific class of pure-feedback nonlinear systems, which involve unknown control directions and input dead-zones [33, 34]. Similarly, an adaptive fuzzy control strategy has been proposed for nonlinear switched systems dealing with failures in sensors [35]. For stochastic non-strict-feedback systems under dead-zone conditions, an adaptive output feedback method has been reported [36]. For fractional-order nonlinear non-strict-feedback large-scale systems with dead-zone input, a decentralized control method has been published [37].

The control methods discussed above are limited as they do not effectively handle external disturbances or dead-zones nonlinearities using echo state networks (ESNs). This limitation motivates an investigation into non-strict-feedback nonlinear systems capable of addressing both challenges simultaneously. In many real-world systems, such as mechanical systems with friction or electronic systems with dead-zones, these issues significantly impact control performance. Therefore, there is a pressing need to explore advanced control techniques that can mitigate the effects of external disturbances and dead-zones. Furthermore, ESN emerges as a promising alternative for functional approximation, offering distinct advantages over other techniques like FLSs or RBFNNs. By leveraging ESNs, we aim to develop an effective control framework that can effectively manage external disturbances and dead-zone nonlinearities.

In comparison to existing research, the primary contributions of this work can be summarized as follows:

- Compared with existing results such as [6, 14, 15] that primarily focus on pure-feedback and strict-feedback nonlinear systems, this study addresses adaptive control for nonlinear systems with a non-strict-feedback structure, dealing with challenges posed by dead-zone nonlinearity and external disturbances.
- In comparison to existing results [7, 19, 38], the use of an ESN stands out due to its ability to approximate unknown functions with continuous online updates to the weights. This characteristic is particularly advantageous in dynamic systems where real-time adjustments are crucial for effective control. Additionally, an adaptive controller designed based on backstepping and ESN approximation further enhances the system's adaptability and effectiveness, making it well-suited for handling nonlinearities and uncertainties.
- The proposed controller ensures that all closed-loop system signals exhibit semi-global uniform ultimate boundedness (SGUUB), guaranteeing convergence of the tracking error to a small neighborhood of the origin. The effectiveness of the proposed control method is substantiated through two simulation examples, including a real-world example about the Brusselator model. Furthermore, the utilization of error assessment criteria in the simulation section provides compelling evidence showcasing the superiority and efficacy of the proposed control approach over existing controllers.

The structure of this work is outlined as follows: In Section 2, a comprehensive system description is provided, and preliminary work is discussed. The design procedure for the controller and the stability analysis of the controlled system are presented in Section 3. To showcase the efficacy of the proposed method, Section 4 presents simulation results. Finally, the paper concludes in Section 5.

Notations. $\mathbb{R}^n$ denotes the Euclidean space, and $\bar{x}_i = [x_1, \ldots, x_i]^T \in \mathbb{R}^i$ with $i = 1, \ldots, n$ and $x =$

$[x_1, \ldots, x_n]^T \in \mathbb{R}^n$ represent state vectors. The functions $f_i(\cdot)$ and $g_i(\cdot)$ are nonlinear functions, where u denotes the system input and y represents the system output. The term $d_i(t)$ denotes the external disturbance.

2. Problem formulation and preliminaries

Consider the following non-strict-feedback nonlinear system with input dead-zone and external disturbance as

$$\begin{cases} \dot{x}_i = g_i(\bar{x}_i)x_{i+1} + f_i(x) + d_i(t), 1 \leq i \leq n-1, \\ \dot{x}_n = g_n(x)u + f_n(x) + d_n(t), \\ y = x_1 \end{cases} \tag{2.1}$$

where $\bar{x}_i = [x_1, \ldots, x_i]^T \in \mathbb{R}^i$ with $i = 1, \ldots, n$, and $x = [x_1, \ldots, x_n]^T \in \mathbb{R}^n$ are state vectors. The functions $fi(\cdot)$ and $g_i(\cdot)$ denote unknown smooth nonlinear functions with $f_i(0) = 0$, and both $fi(\cdot)$ and $g_i(\cdot)$ are locally Lipschitz functions. The variables u and y represent the system input and system output, respectively. Additionally, $d_i(t)$ represents external disturbances, satisfying $|d_i(t)| \leq \bar{d}_i$, where $\bar{d}_i$ is a positive constant.

The nonsymmetric dead-zone [33] with input v and output u is defined as

$$u = \begin{cases} c_r(v - d_r) & \text{if } v \geq d_r, \\ 0 & \text{if } c_l < v < d_r, \\ c_l(v - d_l) & \text{if } v \leq d_l \end{cases} \tag{2.2}$$

where d_r is the right dead-zone break-points and d_l is the left dead-zone break-point, while c_r and c_l represent the slope of the dead-zone.

Controller objectives. The primary objective of this work is to design a controller that ensures the boundedness of all signals in a closed-loop system and guarantees precise tracking of the system output y to the reference signal $y_d(t)$.

2.1. ESN

ESN has proven effective in approximating nonlinearity owing to its exceptional approximation and learning capabilities [19]. The structure comprises three components, illustrated in Figure 1, where K is the number of neurons in the input layer, N is the number of neurons in the hidden layer, and L is the number of neurons in the output layer. The continuous-time state of reservoir neurons is defined as

$$\dot{P}(Z) = -\mu P(Z) + \tanh(W^{\text{in}}\gamma + W_d P(Z) + W_{fb}y) \tag{2.3}$$

where $P(Z)$ represents the activation function of the dynamic reservoir, $\tanh(\cdot)$ is the hyperbolic tangent function, $\mu > 0$ represent the leakage rate of each reservoir neuron, and $W_{in} \in \mathbb{R}^{N\times K}$, $W_d \in \mathbb{R}^{N\times N}$, and $W_{fb} \in \mathbb{R}^{N\times L}$ denote the connection weight matrices for input, internal, and feedback connections, respectively. The u is the external input of dimension K, and the network's output is defined as

$$y = W^T P(Z) \tag{2.4}$$

where $W \in \mathbb{R}^{N\times 1}$ is the output weight matrix.

It has been noted in [19] that there exists an ESN system $y(Z)$ in the form of (2.4) such that for any given continuous function $f(\cdot) : \mathbb{R}^n \to \mathbb{R}$ over a sufficiently large compact set $\Omega \subset \mathbb{R}$, one has

$$\sup_{Z\in\Omega} |f(Z) - y(Z)| \leq \bar{\epsilon} \tag{2.5}$$

where $\bar{\epsilon} > 0$ is an arbitrary positive constant. The function $f(Z)$ is approximate as

$$f(Z) = W^{*T} P(Z) + \epsilon \quad \forall Z \in \Omega \tag{2.6}$$

where ϵ is the approximation error with $|\epsilon| \leq \bar{\epsilon}$, and W^* represents the ideal weight matrix determined as [19]

$$W^* = \arg \min_{W\in\mathbb{R}^{N\times 1}} \left\{ \sup_{Z\in\Omega} |f(Z) - W^{*T} P(Z)| \right\} \tag{2.7}$$

where $P(Z) = [P_1(Z), \ldots, P_n(Z)]^T$ represents the activation function with $P_j(Z)$ chosen in the Gaussian function form as [19]

$$P_j(Z) = \exp\left(-\frac{(Z - \lambda_i)^T (Z - \lambda_i)}{\nu^2} \right), \quad 1 \leq j \leq N \tag{2.8}$$

where $\lambda_i = [\lambda_{j1}, \ldots, \lambda_{iN}]^T$ and ν represent the center and the width of the Gaussian function.

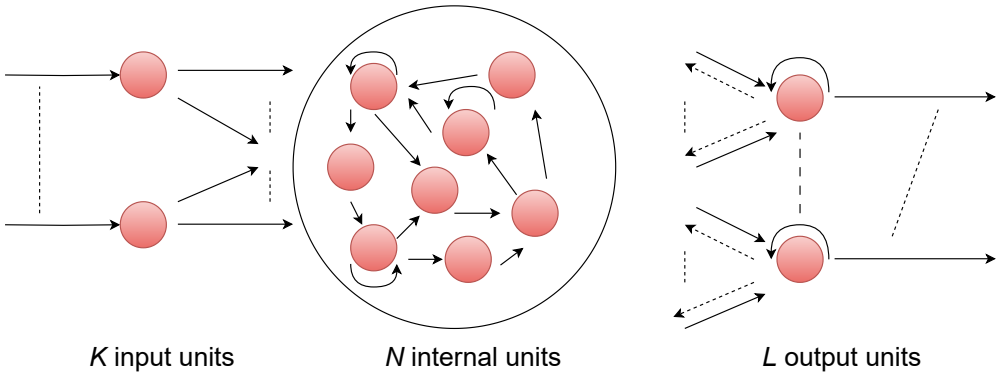

Figure 1. Architecture of ESN.

Remark 2.1. The computational complexity of an ESN is primarily determined by the operations in its hidden layer (reservoir), which have a complexity of $O(N^2)$ due to recurrent connections and nonlinear activations. Additionally, the input layer operation has a complexity of $O(N * K)$, and the output layer operation has a complexity of $O(N * L)$, where K is the number of neurons in the input layer, N is the number of neurons in the hidden layer, and L is the number of neurons in the output layer. Therefore, the overall computational complexity of an ESN is approximately $O(N * K + N^2 + N * L)$, with the reservoir operations typically dominating the complexity. In the special scenario where $L = 1$ and $K = N$, the computational complexity simplifies to $O(N^2)$.

Remark 2.2. ESN stands out as a viable alternative for functional approximation, capable of replacing other techniques like FLSs [19], or RBFNNs [7], or multidimensional Taylor networks (MTN) [38]. Unlike RBFNNs with fixed multilayered feedforward architectures, ESN offers easy and precise training without requiring adjustments to the weights between the input and hidden layers.

Remark 2.3. ESN make training easier by assigning random weights to the input and storage layers, leaving only the output weights to be learned. This simplifies the training procedure while ensuring excellent accuracy in capturing complicated temporal dynamics. In contrast to RBFNNs, which handle static data with localized activations, and rule-based fuzzy logic systems, ESNs excel in sequential data tasks.

Algorithm 1 outlines the sequential procedure for the ESN algorithm:

Algorithm 1 Echo state network (ESN) algorithm

1: **Input:** Set parameters: K, N, L, μ, initialize weight matrices W_{in}, W_d, W_{fb}, and W with small random values
2: **Output:** Trained ESN
3: Initialize reservoir state: $P(Z) = 0$, Gaussian function parameters: λ_i, ν
4: **for** each time step t **do**
5: Compute reservoir state: $\dot{P}(Z) = -\mu P(Z) + \tanh(W^{\text{in}}\gamma + W_d P(Z) + W_{fb} y)$
6: Update state: $P(Z) \leftarrow P(Z) + \Delta t \cdot \dot{P}(Z)$
7: Compute network output: $y = W^T P(Z)$
8: Calculate approximation error: $\delta(Z) = f(Z) - y(Z)$
9: Update output weights: $W^* = \arg\min_{W \in \mathbb{R}^{N\times 1}} \left\{\sup_{Z\in\Omega} |f(Z) - W^T P(Z)|\right\}$
10: **end for**

To facilitate the achievement of the control objective, the following preliminary assumptions and lemma are required:

Assumption 2.1. [6] The reference signal $y_d(t)$ and its nth order derivatives are characterized by continuity and boundedness. Specifically, $\exists$ is a constant $d > 0$ such that the absolute value of $y_d(t)$ is less than or equal to d, i.e., $|y_d(t)| \le d$.

Assumption 2.2. [7] The signs of $g_i(\bar{x}_i)$ for $i = 1, \ldots, n$ are supposed to be known. Generally, we suppose that $g_i(\xi) \ge b_m > 0$, where b_m is a known constant.

Lemma 2.1. (Young's inequality) [1] We have the following inequality for any vectors x and y in $\mathbb{R}^n$

$$xy \le \frac{1}{q} \mid x \mid^q + \frac{1}{r} \mid y \mid^r, \tag{2.9}$$

where $q > 0$ and $r > 0$ are constants with $(q-1)(r-1) = 1$.

Assumption 2.3. [7] The parameters of the dead-zone d_r, d_l, c_r, c_l are not known, but their sign is known, $d_r \ge 0, d_l \le 0, c_r > 0, c_l > 0$, and $\exists$ constants $c_{max} > 0$ and $c_{min} > 0$ are known such that $c_{max} = \max\{c_r, c_l\}$ and $c_{min} = \min\{c_r, c_l\}$.

By employing the input dead-zone as in [33], (2.2) can be represented as

$$u = c(t)v + j(t) \tag{2.10}$$

where

$$c(t) = \begin{cases} c_r & \text{if } v > 0 \\ c_l & \text{if } v \le 0 \end{cases} \tag{2.11}$$

Thus, $j(t)$ can be described as

$$j(t) = \begin{cases} -c_r d_r & \text{if } v \geq d_r, \\ -c(t)v & \text{if } d_l < v < d_r, \\ -c_l d_l & \text{if } v \leq d_l \end{cases} \tag{2.12}$$

From (2.10), we have

$$|j(t)| \leq j^* \tag{2.13}$$

where $j^* = \max\{c_l d_l,\ c_r d_r\}$.

The architecture of the presented control system is demonstrated in Figure 2.

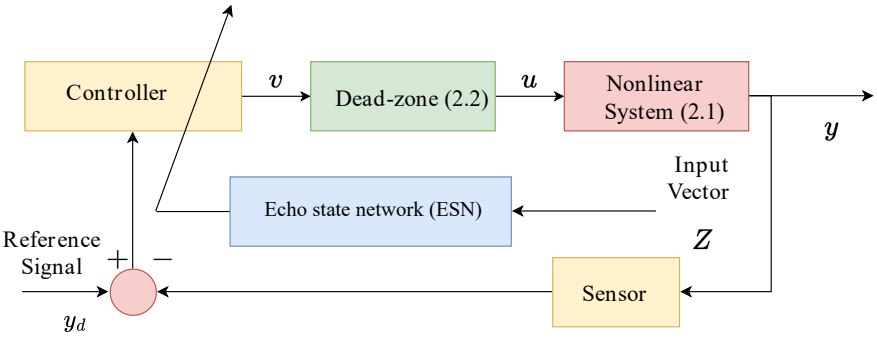

Figure 2. Architecture of control system.

3. Design of adaptive controller and the analysis of stability

In this part, the backstepping technique and ESN are employed to provide an adaptive control method for the non-strict-feedback nonlinear system (2.1). As illustrated below, the recursive backstepping method relies on the introduction of coordinate changes:

$$e_1 = x_1 - y_d \tag{3.1}$$

$$e_i = x_i - \eta_{i-1}; 1 \leq i \leq n-1 \tag{3.2}$$

where $\eta_0 = y_d$ and η_i represents the virtual control law defined as follows:

$$\eta_i = -k_i e_i - \frac{1}{2a_i^2} e_i \hat{\theta}_i P_i^T(X_i) P_i(X_i), \tag{3.3}$$

where $k_i > 0$, $a_i > 0$ are design parameters, $X_i = [\bar{x}_i^T, \bar{\hat{\theta}}_{i-1}^T, \bar{y}_d^{(i)}]^T$ with $\bar{x}_i = [x_1, \cdots, x_i]^T$, and $\hat{\theta}_i$ denotes the estimate of θ_i, which will be provided later.

The control law is chosen as

$$v = -k_n e_n - \frac{1}{2a_n^2} e_n \hat{\theta}_n P_n^T(X_n) P_i(X_n), \tag{3.4}$$

where $k_n > 0$, $a_n > 0$ are design parameters, $X_n = [\bar{x}_n^T, \bar{\hat{\theta}}_{n-1}^T, \bar{y}_d^{(n)}]^T$ with $\bar{x}_n = [x_1, \ldots, x_n]^T$, and $\hat{\theta}_n$ denotes the estimate of θ_n, which will be provided later.

The adaptive law is selected as

$$\dot{\hat{\theta}}_i = \frac{r_i}{2a_i^2} e_i^2 P_i^T(X_i) P_i(X_i) - \sigma_i \hat{\theta}_i, i = 1, \ldots, n \tag{3.5}$$

where $r_i > 0$, $\sigma_i > 0$ are design parameters.
Step 1: From (2.1) and (3.1), we have

$$\dot{e}_1 = g_1 x_2 + f_1 + d_1 - \dot{y}_d. \tag{3.6}$$

As $x_2 = e_2 + \eta_1$, (3.6) becomes

$$\dot{e}_1 = g_1(e_2 + \eta_1) + f_1 + d_1 - \dot{y}_d. \tag{3.7}$$

The Lyapunov function is chosen as

$$V_1 = \frac{1}{2} e_1^2 + \frac{b_m}{2r_1} \tilde{\theta}_1^2, \tag{3.8}$$

where r_1 represents the design parameter, b_m is a constant defined in Assumption 2.2, and $\tilde{\theta}_1 = \theta_1 - \hat{\theta}_1$ represents the estimation error, where $\hat{\theta}_1$ denotes the estimate of θ_1, which will be provided later.
By taking the time derivative of (3.8), we have

$$\begin{aligned} \dot{V}_1 &= e_1(g_1(e_2 + \eta_1) + f_1 + d_1 - \dot{y}_d) - \frac{b_m}{r_1} \tilde{\theta}_1 \dot{\hat{\theta}}_1 \\ &= e_1(\bar{f}_1 + g_1 \eta_1 + d_1) - \frac{b_m}{r_1} \tilde{\theta}_1 \dot{\hat{\theta}}_1 - \frac{1}{2} e_1^2, \end{aligned} \tag{3.9}$$

where $\bar{f}_1 = g_1 e_2 - \dot{y}_d + \frac{1}{2} e_1$. As $\bar{f}_1$ contains unknown functions f_1 and g_1, so an ESN $W_1^T P_1(Z_1)$ is used to approximate it. For $\epsilon_1 > 0$, we have

$$\bar{f}_1 = W_1^T P_1(Z_1) + \delta_1(Z_1), |\delta_1(Z_1)| \leq \epsilon_1, \tag{3.10}$$

where $\delta_1(Z_1)$ is the estimation error, and $Z_1 = [x_1, \ldots, x_n, y_d, \dot{y}_d]^T$.

By using Lemma 2.1, one has

$$\begin{aligned} e_1 \bar{f}_1(Z_1) &= e_1(W_1^{*T} P_1(Z_1) + \delta_1(Z_1)) \\ &\leq \frac{1}{2a_1^2} e_1^2 \|W_1^*\|^2 P_1^T(Z_1) P_1(Z_1) + \frac{a_1^2}{2} + \frac{e_1^2}{2} + \frac{\epsilon_1^2}{2} \\ &\leq \frac{b_m}{2a_1^2} e_1^2 \theta_1 P_1^T(X_1) P_1(X_1) + \frac{a_1^2}{2} + \frac{e_1^2}{2} + \frac{\epsilon_1^2}{2} \end{aligned} \tag{3.11}$$

where $a_1 > 0$ is design parameter, b_m is defined in Assumption 2, and $\theta_1 = \frac{\|W_1^*\|^2}{b_m}$, and $X_1 = [x_1, y_d, \dot{y}_d]^T$.

By using Young's inequality, we have

$$e_1 d_1 \leq \frac{e_1^2}{2} + \frac{\bar{d}_1^2}{2}, \tag{3.12}$$

where $\bar{d}_1 > 0$ is a constant.

Now, by using (3.11), (3.12), virtual control law (3.3), adaptive control law (3.5), and $\tilde{\theta}_1 = \theta_1 - \hat{\theta}$, (3.9) becomes

$$\dot{V}_1 \leq -k_1 b_m e_1^2 + \frac{1}{r_1}\sigma_1 \tilde{\theta}_1 \hat{\theta}_1 + \frac{a_1^2}{2} + \frac{\epsilon_1^2}{2} + + \frac{\bar{d}_1^2}{2}. \tag{3.13}$$

Step i $(2 \leq i \leq n-1)$**:** From (2.1) and (3.2), we have

$$\dot{e}_i = g_i x_{i+1} + f_i + d_i - \eta_{i-1}. \tag{3.14}$$

As $x_{i+1} = e_{i+1} + \eta_i$, (3.14) becomes

$$\dot{e}_i = g_i(e_{i+1} + \eta_i) + f_i + d_i - \dot{\eta}_{i-1} \tag{3.15}$$

The Lyapunov function is described as

$$V_i = \frac{1}{2}e_i^2 + \frac{b_m}{2r_i}\tilde{\theta}_1^2, \tag{3.16}$$

where r_i represents the design parameter, and b_m being a constant shown in Assumption 2.2, $\tilde{\theta}_i = \theta_i - \hat{\theta}_i$ represents the estimation error, where $\hat{\theta}_i$ denotes the estimate of θ_i, which will be provided later.

By taking the time derivative of (3.16), we have

$$\begin{aligned} \dot{V}_i &= e_i(g_i(e_{i+1} + \eta_i) + f_i + d_i - \dot{\eta}_{i-1}) - \frac{b_m}{r_i}\tilde{\theta}_i\dot{\hat{\theta}}_i \\ &= e_i(\bar{f}_i + g_i\eta_i + d_i) - \frac{b_m}{r_i}\tilde{\theta}_i\dot{\hat{\theta}}_i - \frac{1}{2}e_i^2 \end{aligned} \tag{3.17}$$

where $\bar{f}_i = g_i e_{i+1} - \dot{\eta}_{i-1} + \frac{1}{2}e_i$. Since $\bar{f}_1$ includes functions f_i and g_i that are unknown, an ESN $W_i^T P_i(Z_i)$ is used to approximate it. For $\epsilon_i > 0$, we have

$$\bar{f}_i = W_i^T P_i(Z_i) + \delta_i(Z_i), |\delta_i(Z_i)| \leq \epsilon_i, \tag{3.18}$$

with $\delta_i(Z_i)$ being the estimation error, and $Z_i = [x_1, \ldots x_n, \bar{\hat{\theta}}_{i-1}^T, \bar{y}_d^{(i)}]^T$ with $\bar{\hat{\theta}}_{i-1}^T = [\hat{\theta}_1, \ldots, \hat{\theta}_{i-1}]^T$ and $\bar{y}_d^{(i)}]^T = [y_d, \cdots, y_d^{(i)}]^T$, respectively.

Similarly to (3.11), one has

$$\begin{aligned} e_i\bar{f}_i(Z_i) &= e_i(W_i^{*T}P_i(Z_i) + \delta_i(Z_i)) \\ &\leq \frac{1}{2a_i^2}e_i^2\|W_i^*\|^2 P_i^T(Z_i)P_i(Z_i) + \frac{a_i^2}{2} + \frac{e_i^2}{2} + \frac{\epsilon_i^2}{2} \\ &\leq \frac{b_m}{2a_i^2}z_i^2\theta_i P_i^T(X_i)P_i(X_i) + \frac{a_i^2}{2} + \frac{e_i^2}{2} + \frac{\epsilon_i^2}{2} \end{aligned} \tag{3.19}$$

where b_m is defined in Assumption 2, $a_i > 0$ is a design parameter, and $\theta_i = \frac{\|W_i^*\|^2}{b_m}$, and $X_i = [\bar{x}_i^T, \bar{\hat{\theta}}_{i-1}^T, \bar{y}_d^{(i)}]^T$ with $\bar{x}_i = [x_1, \cdots, x_i]^T$.

Using Lemma 2.1, one has

$$e_i d_i \leq \frac{e_i^2}{2} + \frac{\bar{d}_i^2}{2}, \tag{3.20}$$

where $\bar{d}_i > 0$ is a constant.

Now, by using (3.19), (3.20), virtual control law (3.3), adaptive control law (3.5), and $\tilde{\theta}_i = \theta_i - \hat{\theta}_i$, (3.17) becomes

$$\dot{V}_i \leq -k_i b_m e_i^2 + \frac{1}{r_i}\sigma_i \tilde{\theta}_i \hat{\theta}_i + \frac{a_i^2}{2} + \frac{\epsilon_i^2}{2} + \frac{\bar{d}_i^2}{2}. \tag{3.21}$$

Step *n*: From (2.1), (2.10), and (3.2), we have

$$\begin{aligned} \dot{e}_n &= g_n u + f_n + d_n - \eta_{n-1} \\ &= g_n(c(t)v + j(t)) + f_n + d_n - \eta_{n-1} \end{aligned} \tag{3.22}$$

The Lyapunov function candidate is represented as

$$V_n = \frac{1}{2}e_n^2 + \frac{b_m}{2r_n}\tilde{\theta}_n^2, \tag{3.23}$$

where r_i denotes the design parameter, and b_m being a constant shown in Assumption 2.2, $\tilde{\theta}_n = \theta_n - \hat{\theta}_n$ represents the estimation error, where $\hat{\theta}_n$ denotes the estimate of θ_n, which will be provided later.

By taking the time derivative of (3.23), we have

$$\begin{aligned} \dot{V}_n &= e_n g_n(c(t)v + j(t)) + e_n f_n + e_n d_n - e_n \dot{\eta}_{n-1} - \frac{b_m}{r_n}\tilde{\theta}_n \dot{\hat{\theta}}_n \\ &= e_n g_n(c(t)v + j(t)) + e_n \bar{f}_n + e_n d_n - \frac{b_m}{r_n}\tilde{\theta}_n \dot{\hat{\theta}}_n - \frac{1}{2}e_n^2 \end{aligned} \tag{3.24}$$

where $\bar{f}_n = f_n - \dot{\eta}_{n-1} + \frac{1}{2}e_n$. As $\bar{f}_n$ contains an unknown function f_n , an ESN $W_n^T P_n(Z_n)$ is used to approximate it. For $\epsilon_n > 0$, we have

$$\bar{f}_n = W_n^T P_n(Z_n) + \delta_n(Z_n), |\delta_n(Z_n)| \leq \epsilon_n. \tag{3.25}$$

where $\delta_n(Z_n)$ is the estimation error, and $Z_n = [x_1, \ldots, x_n, \bar{\hat{\theta}}_{n-1}^T, \bar{y}_d^{(n)}]^T$ with $\bar{\hat{\theta}}_{n-1}^T = [\hat{\theta}_1, \ldots, \hat{\theta}_{n-1}]^T$ and $\bar{y}_d^{(n)}]^T = [y_d, \ldots, y_d^{(n)}]^T$, respectively.

By using Lemma 2.1, one has

$$\begin{aligned} e_n \bar{f}_n(Z_n) &= e_n(W_n^{*T} P_n(Z_n) + \delta_n(Z_n)) \\ &\leq \frac{1}{2a_n^2} e_n^2 \|W_n^*\|^2 P_n^T(Z_n) P_n(Z_n) + \frac{a_n^2}{2} + \frac{e_n^2}{2} + \frac{\epsilon_n^2}{2} \\ &\leq \frac{b_m}{2a_n^2} e_n^2 \theta_n P_n^T(X_n) P_n(X_n) + \frac{a_n^2}{2} + \frac{e_n^2}{2} + \frac{\epsilon_n^2}{2} \end{aligned} \tag{3.26}$$

where $\theta_n = \frac{\|W_i^*\|^2}{b_m}$, $X_n = [\bar{x}_n^T, \bar{\hat{\theta}}_{n-1}^T, \bar{y}_d^{(n)}]^T$ with $\bar{x}_n = [x_1, \ldots, x_n]^T$, and $a_n > 0$ is the design parameter.

By using Young's inequality, one has

$$e_n d_n \leq \frac{e_n^2}{2} + \frac{\bar{d}_n^2}{2}, \tag{3.27}$$

where $\bar{d}_n > 0$ is a constant.

Now, by using (2.13), (3.26), (3.27), real control law (3.4), adaptive control law (3.5), and $\tilde{\theta}_i = \theta_i - \hat{\theta}_i$, (3.24) becomes

$$\dot{V}_n \leq -k_n b_m e_n^2 + \frac{1}{r_n}\sigma_n \tilde{\theta}_n \hat{\theta}_n + \frac{a_n^2}{2} + \frac{\epsilon_n^2}{2} + \frac{\bar{d}_n^2}{2} + \frac{1}{2}j^{*^2}. \tag{3.28}$$

Theorem 3.1. Consider the nonlinear system (2.1) with dead-zone nonlinearity (2.2) under Assumptions 2.1–2.3. Assume that ESN can effectively approximate each unknown function $\bar{f}_i$ with $1 \leq i \leq n$, ensuring that the approximation errors δ_i are bounded. Under the real controller (3.4), virtual control law (3.3) and the adaptive law (3.5) with bounded initial conditions, the proposed controller demonstrates that all signals in the closed-loop system are SGUUB. In addition, the tracking error e_1 converges to a confined region around the origin.

Proof. Define $V = \sum_{i=1}^{n} V_i$. It follows from (3.13), (3.21), and (3.28) that

$$\dot{V} \leq -\sum_{i=1}^{n} k_i b_m e_i^2 + \sum_{i=1}^{n} \frac{1}{r_i}\sigma_i \tilde{\theta}_i \hat{\theta}_i + \sum_{i=1}^{n}\left(\frac{a_i^2}{2} + \frac{\epsilon_i^2}{2} + \frac{\bar{d}_i^2}{2}\right) + \frac{1}{2}j^{*^2}. \tag{3.29}$$

since

$$\tilde{\theta}_i \hat{\theta}_i = \tilde{\theta}_i(\theta_i - \tilde{\theta}_i) \leq -\frac{1}{2}\tilde{\theta}_i^2 + \frac{1}{2}\theta_i^2. \tag{3.30}$$

Therefore, (3.29) can be written as

$$\begin{aligned} \dot{V} &\leq -a_0\left(\sum_{i=1}^{n}\frac{1}{2}e_i^2 + \sum_{i=1}^{n}\frac{b_m}{2r_i}\tilde{\theta}_i^2\right) + b_0 \\ &\leq -a_0 V + b_0, \end{aligned} \tag{3.31}$$

where $a_0 = \min\{2k_i b_m, \sigma_i | 1 \leq i \leq n$ and $b_0 = \sum_{i=1}^{n}\left(\frac{a_i^2}{2} + \frac{\epsilon_i^2}{2} + \frac{\bar{d}_i^2}{2}\right) + \frac{1}{2}j^{*^2}$.

Equation (3.31) implies that in the closed-loop system, all signals are bounded.

Remark 3.1. The performance of the controller is greatly impacted by the design parameters k_i, b_i, r_i, and σ_i. Tracking errors are decreased by reducing a_i while increasing k_i and σ_i, but control law complexity is increased. Choosing the right control parameters is crucial for meeting system requirements. Carefully tuning these parameters through the trial and error method involves closely watching how the controller performs. This way, the controller can balance between reducing tracking errors and keeping the control law manageable.

Remark 3.2. In our comparative analysis, it is worth noting that the existing method [1] did not account for the influence of nonlinearity and external disturbance in the control approach, which is crucial as nonlinearity can significantly impact system performance. Furthermore, in contrast to our proposed work, [6] focuses on pure-feedback nonlinear systems, while our approach addresses the more complex non-strict-feedback nonlinear systems. Additionally, [11] deals with saturation nonlinearity, whereas in practical systems, the presence of dead-zones nonlinearity poses a more challenging scenario. These distinctions underscore the unique contributions and practical relevance of our proposed methodology.

Remark 3.3. In [39], the authors proposed adaptive control for nonlinear systems with input saturation using FLSs, while in [40] NNs were employed for tracking control of nonlinear systems under saturation via command filters. Both approaches primarily address saturation nonlinearity. In contrast, this paper utilizes ESNs to tackle the more complex challenges posed by dead-zone nonlinearity and

external disturbances in non-strict-feedback nonlinear systems. By randomly assigning weights in the input and storage layers and training only the output weights, ESNs simplify the training process and achieve high accuracy in capturing complex temporal dynamics.

4. Simulation results

Example 4.1. Consider the following non-strict-feedback nonlinear system as

$$\begin{cases} \dot{x}_1 = x_1 x_2^2 + x_1^2 \sin(x_2) + (1.5 + 0.5\sin(x_1))x_2 + 0.5\cos(t) \\ \dot{x}_2 = x_1^2 x_2 e^{x_2} + x_1 \cos(x_1 x_2) + (1.5 + \sin(x_1 x_2))u + \sin(0.5t) \\ y = x_1 \end{cases} \tag{4.1}$$

where $f_1 = x_1 x_2^2 + x_1^2 \sin(x_2)$, $f_2 = x_1^2 x_2 e^{x_2} + x_1 \cos(x_1 x_2)$, $g_1 = 1.5 + 0.5\sin(x_1)$, $g_2 = 1.5 + \sin(x_1 x_2)$, $d_1(t) = 0.5\cos(t)$, $d_2(t) = \sin(0.5t)$. The reference signal is given as $y_d = 0.5(\sin(t) + \sin(0.5t))$.

The virtual control law η_1, actual control law v, and adaptive laws are chosen as

$$\eta_1 = -k_1 e_1 - \frac{1}{2a_1^2} e_1 \hat{\theta}_1 P_1^T(Z_1) P_1(Z_1), \tag{4.2}$$

$$v = -k_2 e_2 - \frac{1}{2a_2^2} e_2 \hat{\theta}_2 P_2^T(Z_2) P_2(Z_2), \tag{4.3}$$

$$\dot{\hat{\theta}}_i = \frac{r_i}{2a_i^2} e_i^2 P_i^T(Z_i) P_i(Z_i) - \sigma_i \hat{\theta}_i, i = 1, 2 \tag{4.4}$$

The parameters are selected as $k_1 = 6, k_2 = 10$, $a_1 = 1, a_2 = 1$, $r_1 = 3, r_2 = 3$, $\sigma_1 = 0.05, \sigma_2 = 0.05$. The initial conditions are chosen as $x_1(0) = 0.5, x_2(0) = 0$, $\hat{\theta}_1(0) = 0, \hat{\theta}_2(0) = 0$. The dead-zone parameters are chosen as $d_r = 0.5, d_l = -0.6, c_r = 1, c_l = 1.2$. The center vectors and widths chosen for the Gaussian function are represented as $\lambda_i = [-1, -0.5, 0, 0.5, 1]$ and $\nu = 2$. The simulation results are illustrated in Figures 3–7, providing a detailed analysis of the system's performance. Figure 3 presents the system output $y = x_1$ alongside the reference signal y_d, demonstrating the effective tracking performance achieved under the proposed control method. Figure 4 visually represents the tracking error e_1, showing its convergence around a small region near the origin. Furthermore, Figure 5 offers insights into the state variable x_2, indicating its bounded behavior. Both the control signal v and system input u are illustrated as bounded in Figure 6. Additionally, Figure 7 showcases the boundedness of the adaptive laws. The simulation results confirm that the designed controller is suitable for achieving precise tracking performance and ensuring the boundedness of all closed-loop signals in nonlinear systems, particularly in the presence of external disturbances and input dead-zone.

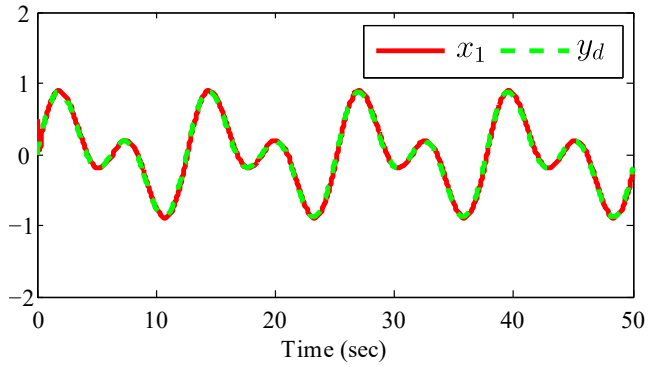

Figure 3. The trajectories of x_1 and y_d for example 4.1.

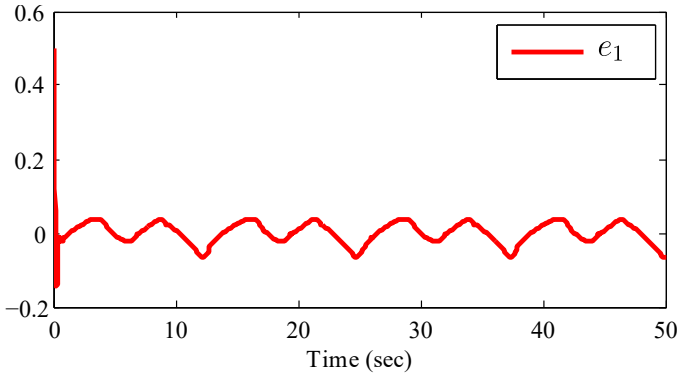

Figure 4. The trajectory of tracking error e_1 for example 4.1.

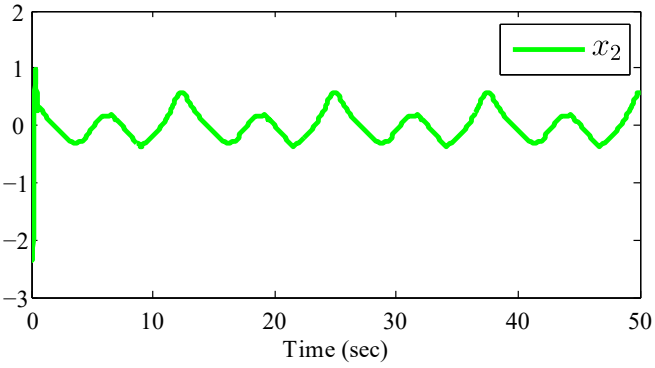

Figure 5. The trajectory of system state x_2 for example 4.1.

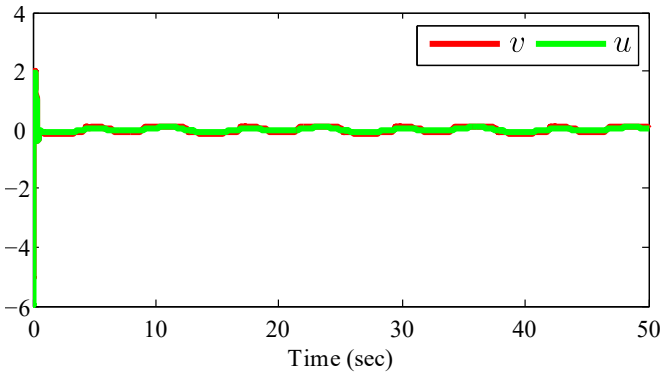

Figure 6. The trajectories of control signal v and system input u for example 4.1.

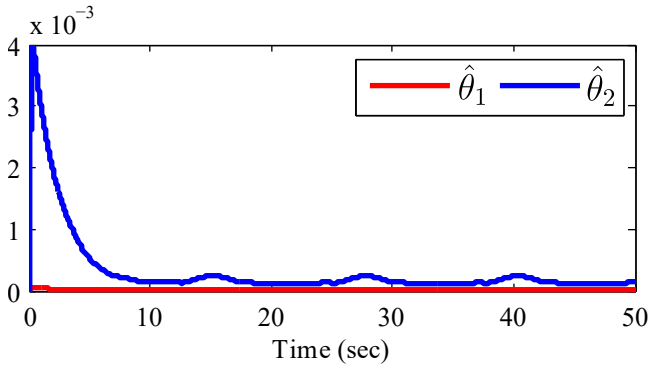

Figure 7. The trajectories of adaptive laws $\hat{\theta}_1$ and $\hat{\theta}_2$ for example 4.1.

Moreover, to validate the superiority of the proposed control schemes over the existing RBFNN controller [7], MTN controller [38], and fuzzy controller [19] for this particular system, a comparative analysis is conducted using assessment error criteria. For a given pair of data points $(y_i(t), y_{id}(t))$ in the interval $t \in [1, P]$, Table 1 displays the assessment error criteria.

Table 1. Comparison of tracking performance using different error calculations for example 1.

Error	Proposed ESN controller	RBFNN controller [7]	MTN controller [38]	Fuzzy controller [19]
J_{SSE}	10.1599	9.5166	9.7184	9.6039
J_{MAE}	0.5000	0.5000	0.5000	0.5000
J_{NMSE}	0.0204	0.0210	0.0203	0.0256
J_{BFR}	99.98%	99.98%	99.98%	99.97%
J_{MSE}	0.0061	0.0064	0.0062	0.0081
J_{RMSE}	0.0778	0.0799	0.0788	0.0899

Sum of squared error (SSE): $J_{SSE} = \sum_{t=1}^{P}(y_i(t) - y_{id}(t))^2$; maximum absolute error (MAE): $J_{MAE} =$

$\max_{1\le t\le P}|y_i(t)-y_{id}(t)|$; normalized mean squared error (NMSE): $J_{NMSE}=\frac{\sum_{t=1}^{P}(y_i(t)-y_{id}(t))^2}{\sum_{t=1}^{P}(y_i(t)-\bar{y_{id}})^2}$; best fit rate (BFR): $J_{BFR}=1-\frac{\sum_{t=1}^{P}(y_i(t)-y_{id}(t))^2}{\sum_{t=1}^{P}(y_i(t)-\bar{y_{id}})^2}\times 100\%$; mean squared error (MSE): $J_{MSE}=\frac{\sum_{t=1}^{P}(y_i(t)-y_{id})^2}{P}$; root mean squared error (RMSE): $J_{RMSE}=\sqrt{\frac{1}{P}\sum_{t=1}^{P}(y_i(t)-y_{id}(t))^2}$ where $\bar{y_{id}}$ represents the mean of $y_{id}(t)$.

The results presented in Table 1 reveal a marginal improvement in the proposed control scheme compared to the RBFNN controller [7], MTN controller [38], and fuzzy controller [19] for this particular system. This improvement serves as evidence for the effectiveness of our proposed control method.

Example 4.2. In this example, a real-world application of the Brusselator model is used to show the efficacy of the proposed strategy. A simplified Brusselator model describes a specific group of chemical reactions [41]

$$\begin{cases}\dot{x}_1 = a-(b+1)x_1+x_1^2x_2+0.5\cos(t)\\ \dot{x}_2 = bx_1-x_1^2x_2+(2+\cos x_1)u+\sin(0.5t)\\ y=x_1\end{cases} \tag{4.5}$$

where $f_1=a-(b+1)x_1$, $f_2=bx_1-x_1^2x_2$, $g_1=x_1^2$, $g_2=2+\cos x_1$, $d_1(t)=0.5\cos(t)$, $d_2(t)=\sin(0.5t)$. The reference signal is given as $y_d=0.5(\sin(t)$.

The virtual control law η_1, actual control law v, and adaptive laws are chosen as

$$\eta_1=-k_1e_1-\frac{1}{2a_1^2}e_1\hat{\theta}_1P_1^T(Z_1)P_1(Z_1), \tag{4.6}$$

$$v=-k_2e_2-\frac{1}{2a_2^2}e_2\hat{\theta}_2P_2^T(Z_2)P_2(Z_2), \tag{4.7}$$

$$\dot{\hat{\theta}}_i=\frac{r_i}{2a_i^2}e_i^2P_i^T(Z_i)P_i(Z_i)-\sigma_i\hat{\theta}_i, i=1,2 \tag{4.8}$$

The parameters are $a=1$, $b=3$, $k_1=10, k_2=10$, $a_1=1, a_2=1$, $r_1=3, r_2=3$, and $\sigma_1=0.05, \sigma_2=0.05$. The initial conditions are set as $x_1(0)=0.4, x_2(0)=0.4$, and $\hat{\theta}_1(0)=0, \hat{\theta}_2(0)=0$. The dead-zone parameters are set at $d_r=0.5, d_l=-0.6, c_r=1, c_l=1.2$. The center vectors and widths chosen for the Gaussian function are represented as $\lambda_i=[-1,-0.5,0,0.5,1]$ and $\nu=2$. The simulation results are depicted in Figures 8–12, offering an intricate analysis of the system performance. Figure 8 showcases the system output $y=x_1$ alongside the reference signal y_d, highlighting the effective tracking performance achieved with the proposed control method. Moving on, Figure 9 visually represents the tracking error e_1, depicting its convergence around a small region near the origin. Furthermore, Figure 10 provides insights into the behavior of the state variable x_2, indicating its bounded nature. Both the control signal v and system input u are shown to be bounded in Figure 11. Additionally, Figure 12 showcases the boundedness of the adaptive laws. These simulation results affirm that the designed controller is adept at achieving precise tracking performance and ensuring the boundedness of all closed-loop signals in nonlinear systems, especially when confronted with external disturbances and input dead-zone.

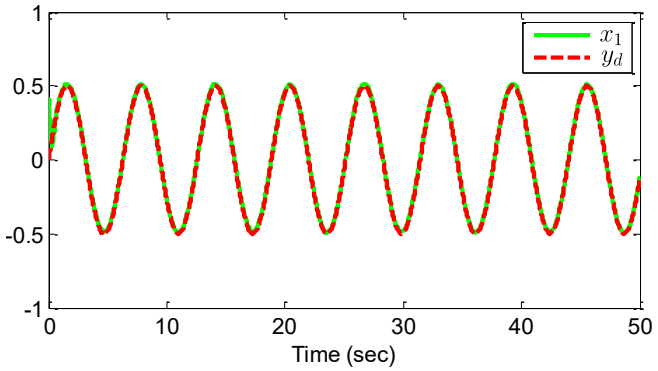

Figure 8. The trajectories of x_1 and y_d for example 4.2.

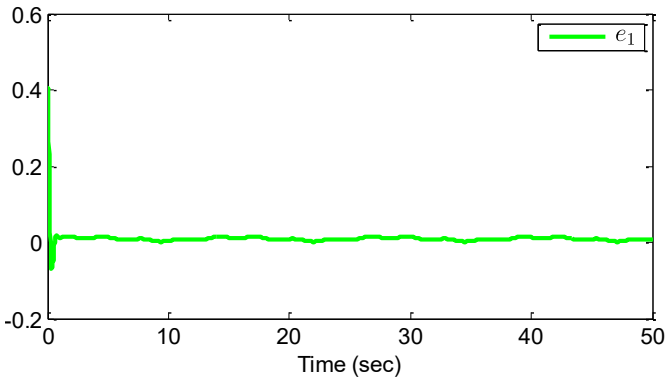

Figure 9. The trajectory of tracking error e_1 for example 4.2.

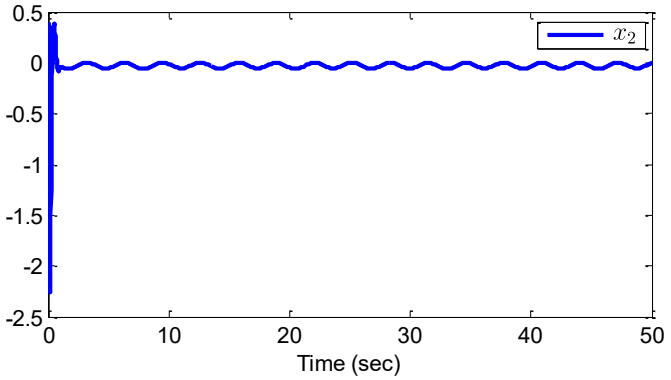

Figure 10. The trajectory of system state x_2 for example 4.2.

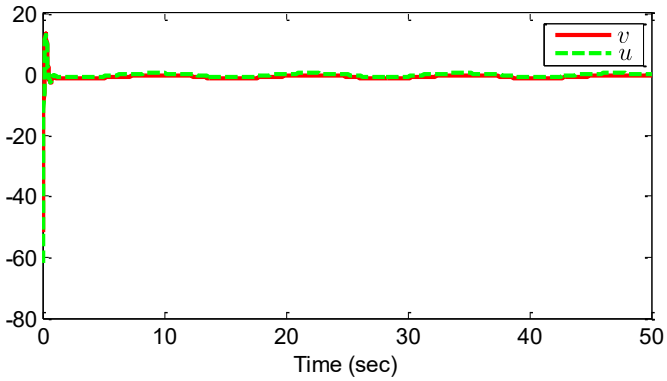

Figure 11. The trajectories of control signal v and system input u for example 4.2.

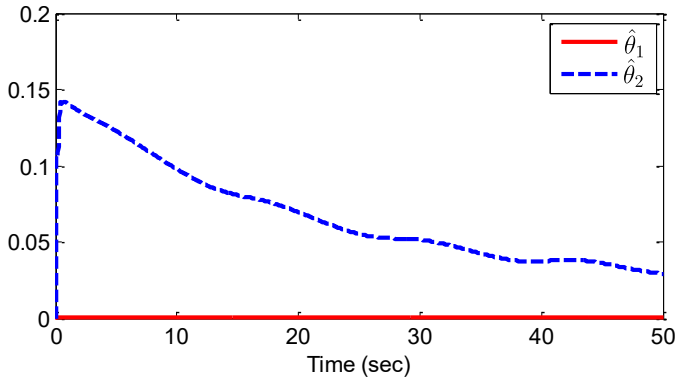

Figure 12. The trajectories of adaptive laws $\hat{\theta}_1$ and $\hat{\theta}_2$ for example 4.2.

To validate the superiority of the proposed control scheme over the existing RBFNN controller [7], MTN controller [38], and fuzzy controller [19] for this specific system, a comparative analysis is conducted using assessment error criteria defined in Example 1. Table 2 shows that the suggested control strategy performs marginally better than the RBFNN controller [7], MTN controller [38], and fuzzy controller [19] for this system. This improvement supports the effectiveness of our proposed control mechanism.

Table 2. Comparison of tracking performance using different error calculations for example 4.2.

Error	Proposed ESN controller	RBFNN controller [7]	MTN controller [38]	Fuzzy controller [19]
J_{SSE}	9.1599	8.5166	8.7184	8.6039
J_{MAE}	0.4500	0.4500	0.4500	0.4500
J_{NMSE}	0.0184	0.0190	0.0183	0.0236
J_{BFR}	99.97%	99.97%	99.97%	99.96%
J_{MSE}	0.0051	0.0054	0.0052	0.0071
J_{RMSE}	0.0718	0.0739	0.0728	0.0839

5. Conclusions

This study addresses adaptive control for non-strict-feedback nonlinear systems with dead-zone and external disturbances. It uses an ESN to approximate the unknown nonlinear function and designs an adaptive controller using the backstepping method and Lyapunov analysis with ESN approximation. The proposed controller ensures SGUUB of all signals in the closed-loop system, as shown through a thorough Lyapunov stability analysis. Two examples and error assessment criteria validate the method's effectiveness. However, it's important to note that the tuning of control parameters through the trial and error method can be time-consuming, which serves as a limitation of the approach. In future research work, our focus will extend to stochastic nonlinear systems incorporating input quantization.

Author Contributions

Hadil Alhazmi: Writing–original draft, Resources, Methodology; Mohamed Kharrat: Conceptualization, Methodology, Writing–review & editing. All authors have reviewed the results and approved the final version of the manuscript.

Use of AI tools declaration

The authors declare they have not used Artificial Intelligence (AI) tools in creating this article.

Acknowledgments

This work was funded by the Princess Nourah bint Abdulrahman University Researchers Supporting Project number (PNURSP2024R528), Princess Nourah bint Abdulrahman University, Riyadh, Saudi Arabia.

Conflict of interest

The authors confirm no conflicts of interest.

References

1. B. Ren, S. S. Ge, K. P. Tee, T. H. Lee, Adaptive neural control for output feedback nonlinear systems using a barrier Lyapunov function, *IEEE Trans. Neural Netw.*, **21** (2010), 1339–1345. https://doi.org/10.1109/TNN.2010.2047115
2. A. Kamalifar, M. B. Menhaj, M. N. Monfared, A. Fakharian, Design of robust model reference adaptive controller for a wider class of nonlinear systems, *Iran. J. Sci. Technol. Trans. Electr. Eng.*, **46** (2022), 127–139. https://doi.org/10.1007/s40998-021-00451-8
3. B. Chen, H. Zhang, C. Lin, Observer-based adaptive neural network control for nonlinear systems in nonstrict-feedback form, *IEEE Trans. Neural Netw. Learn. Syst.*, **27** (2016), 89–98. https://doi.org/10.1109/TNNLS.2015.2412121

4. M. Kharrat, M. Krichen, L. Alkhalifa, K. Gasmi, Neural networks-based adaptive command filter control for nonlinear systems with unknown backlash-like hysteresis and its application to single link robot manipulator, *AIMS Math.*, **9** (2024), 959–973. https://doi.org/10.3934/math.2024048
5. C. Wang, M. Liang, Y. Chai, An adaptive control of fractional-order nonlinear uncertain systems with input saturation, *Complexity*, **2019** (2019), 5643298. https://doi.org/10.1155/2019/5643298
6. M. Wang, X. Liu, P. Shi, Adaptive neural control of pure-feedback nonlinear time-delay systems via dynamic surface technique, *IEEE Trans. Syst. Man Cybern. B*, **41** (2011), 1681–1692. https://doi.org/10.1109/TSMCB.2011.2159111
7. M. Kharrat, M. Krichen, L. Alkhalifa, K. Gasmi, Neural-networks-based adaptive fault-tolerant control of nonlinear systems with actuator faults and input quantization, *IEEE Access*, **11** (2023), 137680–137687. https://doi.org/10.1109/ACCESS.2023.3338376
8. J. An, W. Yang, X. Xu, T. Chen, B. Du, Y. Tang, et al., Decentralized adaptive control for quasi-consensus in heterogeneous nonlinear multiagent systems, *Discrete Dyn. Nat. Soc.*, **2021** (2021), 2230805. https://doi.org/10.1155/2021/2230805
9. S. Tong, T. Wang, Y. Li, H. Zhang, Adaptive neural network output feedback control for stochastic nonlinear systems with unknown dead-zone and unmodeled dynamics, *IEEE Trans. Cybern.*, **44** (2014), 910–921. https://doi.org/10.1109/TCYB.2013.2276043
10. J. Luo, H. Liu, Adaptive fractional fuzzy sliding mode control for multivariable nonlinear systems, *Discrete Dyn. Nat. Soc.*, **2014** (2014), 541918. https://doi.org/10.1155/2014/541918
11. Q. Zhou, H. Li, C. Wu, L. Wang, C. K. Ahn, Adaptive fuzzy control of nonlinear systems with unmodeled dynamics and input saturation using small-gain approach, *IEEE Trans. Syst. Man Cybern.: Syst.*, **47** (2017), 1979–1989. https://doi.org/10.1109/TSMC.2016.2586108
12. B. Chen, X. Liu, K. Liu, C. Lin, Fuzzy approximation-based adaptive control of nonlinear delayed systems with unknown dead zone, *IEEE Trans. Fuzzy Syst.*, **22** (2014), 237–248. https://doi.org/10.1109/TFUZZ.2013.2250507
13. G. Chen, J. Dong, Approximate optimal adaptive prescribed performance control for uncertain nonlinear systems with feature information, *IEEE Trans. Syst. Man Cybern.: Syst.*, **54** (2024), 2298–2308. https://doi.org/10.1109/TSMC.2023.3342854
14. Y. Deng, X. Zhang, G. Zhang, X. Han, Adaptive neural tracking control of strict-feedback nonlinear systems with event-triggered state measurement, *ISA Trans.*, **117** (2021), 28–39. https://doi.org/10.1016/j.isatra.2021.01.049
15. S. Tong, X. Min, Y. Li, Observer-based adaptive fuzzy tracking control for strict-feedback nonlinear systems with unknown control gain functions, *IEEE Trans. Cybern.*, **50** (2020), 3903–3913. https://doi.org/10.1109/TCYB.2020.2977175
16. G. Yang, J. Yao, Multilayer neurocontrol of high-order uncertain nonlinear systems with active disturbance rejection, *Int. J. Robust Nonlinear Control*, **34** (2024), 2972–2987. https://doi.org/10.1002/rnc.7118
17. G. Yang, Asymptotic tracking with novel integral robust schemes for mismatched uncertain nonlinear systems, *Int. J. Robust Nonlinear Control*, **33** (2023), 1988–2002. https://doi.org/10.1002/rnc.6499
18. C. C. Ku, K. Y. Lee, Diagonal recurrent neural networks for dynamic systems control, *IEEE Trans. Neural Netw.*, **6** (1995), 144–156. https://doi.org/10.1109/72.363441

19. S. Lun, M. Wu, X. Lu, M. Li, Fixed-time adaptive tracking control for MIMO nonlinear system with input delay saturation based on echo state network, *IET Control Theory Appl.*, **18** (2024), 374–383. https://doi.org/10.1049/cth2.12559
20. S. I. Han, J. M. Lee, Precise positioning of nonsmooth dynamic systems using fuzzy wavelet echo state networks and dynamic surface sliding mode control, *IEEE Trans. Ind. Electron.*, **60** (2013), 5124–5136. https://doi.org/10.1109/TIE.2012.2218560
21. Y. Wang, G. Zong, D. Yang, K. Shi, Finite-time adaptive tracking control for a class of nonstrict feedback nonlinear systems with full state constraints, *Int. J. Robust Nonlinear Control*, **32** (2022), 2551–2569. https://doi.org/10.1002/rnc.5777
22. N. Xu, X. Zhao, G. Zong, Y. Wang, Adaptive control design for uncertain switched nonstrict-feedback nonlinear systems to achieve asymptotic tracking performance, *Appl. Math. Comput.*, **408** (2021), 126344. https://doi.org/10.1016/j.amc.2021.126344
23. J. Wu, Y. Hu, Y. Huang, Indirect adaptive robust control of nonstrict feedback nonlinear systems by a fuzzy approximation strategy, *ISA Trans.*, **108** (2021), 10–17. https://doi.org/10.1016/j.isatra.2020.08.038
24. Y. Li, S. Tong, Command-filtered-based fuzzy adaptive control design for MIMO-switched nonstrict-feedback nonlinear systems, *IEEE Trans. Fuzzy Syst.*, **25** (2017), 668–681. https://doi.org/10.1109/TFUZZ.2016.2574913
25. M. Kharrat, Neural networks-based adaptive fault-tolerant control for stochastic nonlinear systems with unknown backlash-like hysteresis and actuator faults, *J. Appl. Math. Comput.*, **70** (2024), 1995–2018. https://doi.org/10.1007/s12190-024-02042-2
26. S. Sui, C. P. Chen, S. Tong, Event-trigger-based finite-time fuzzy adaptive control for stochastic nonlinear system with unmodeled dynamics, *IEEE Trans. Fuzzy Syst.*, **29** (2021), 1914–1926. https://doi.org/10.1109/TFUZZ.2020.2988849
27. Y. Alruwaily, M. Kharrat, Funnel-based adaptive neural fault-tolerant control for nonlinear systems with dead-zone and actuator faults: application to rigid robot manipulator and inverted pendulum systems, *Complexity*, in press. https://doi.org/10.1155/2024/5344619
28. T. Gao, T. Li, Y. J. Liu, S. Tong, F. Sun, Observer-based adaptive fuzzy control of non-strict feedback nonlinear systems with function constraints, *IEEE Trans. Fuzzy Syst.*, **31** (2023), 2556–2567. https://doi.org/10.1109/TFUZZ.2022.3228319
29. Y. Liang, Y. X. Li, W. W. Che, Z. Hou, Adaptive fuzzy asymptotic tracking for nonlinear systems with nonstrict-feedback structure, *IEEE Trans. Cybern.*, **51** (2021), 853–861. https://doi.org/10.1109/TCYB.2020.3002242
30. X. Zhao, P. Shi, X. Zheng, L. Zhang, Adaptive tracking control for switched stochastic nonlinear systems with unknown actuator dead-zone, *Automatica*, **60** (2015), 193–200. https://doi.org/10.1016/j.automatica.2015.07.022
31. M. Cai, P. Shi, J. Yu, Adaptive neural finite-Time control of non-strict feedback nonlinear systems with non-symmetrical dead-zone, *IEEE Trans. Neural Netw. Learn. Syst.*, **35** (2024), 1409–1414. https://doi.org/10.1109/TNNLS.2022.3178366
32. K. Li, S. Tong, Observer-based finite-time fuzzy adaptive control for MIMO non-strict feedback nonlinear systems with errors constraint, *Neurocomputing*, **341** (2019), 135–148. https://doi.org/10.1016/j.neucom.2019.02.022

33. H. Wang, H. R. Karimi, P. X. Liu, H. Yang, Adaptive neural control of nonlinear systems with unknown control directions and input dead-zone, *IEEE Trans. Syst. Man Cybern.: Syst.*, **48** (2018), 1897–1907. https://doi.org/10.1109/TSMC.2017.2709813
34. J. Ni, Z. Wu, L. Liu, C. Liu, Fixed-time adaptive neural network control for nonstrict-feedback nonlinear systems with deadzone and output constraint, *ISA Trans.*, **97** (2020), 458–473. https://doi.org/10.1016/j.isatra.2019.07.013
35. J. Zhang, S. Li, Z. Xiang, Adaptive fuzzy output feedback event-triggered control for a class of switched nonlinear systems with sensor failures, *IEEE Trans. Circuits Syst. I*, **67** (2020), 5336–5346. https://doi.org/10.1109/TCSI.2020.2994547
36. Y. Sun, B. Mao, H. Liu, S. Zhou, Output feedback adaptive control for stochastic non-strict-feedback system with dead-zone, *Int. J. Control Autom. Syst.*, **18** (2020), 2621–2629. https://doi.org/10.1007/s12555-019-0876-9
37. Y. Zhan, X. Li, S. Tong, Observer-based decentralized control for non-strict-feedback fractional-order nonlinear large-scale systems with unknown dead zones, *IEEE Trans. Neural Netw. Learn. Syst.*, **34** (2023), 7479–7490. https://doi.org/10.1109/TNNLS.2022.3143901
38. S. Zhu, L. Chu, M. Wang, Y. Han, S. Yang, Multi-dimensional Taylor network-based adaptive output-feedback tracking control for a class of nonlinear systems, *IEEE Access*, **8** (2020), 77298–77307. https://doi.org/10.1109/ACCESS.2020.2989523
39. J. Liu, Q. G. Wang, J. Yu, Convex optimization-based adaptive fuzzy control for uncertain nonlinear systems with input saturation using command filtered backstepping, *IEEE Trans. Fuzzy Syst.*, **31** (2023), 2086–2091. https://doi.org/10.1109/TFUZZ.2022.3216103
40. J. Liu, Q. G. Wang, J. Yu, Event-triggered adaptive neural network tracking control for uncertain systems with unknown input saturation based on command filters, *IEEE Trans. Neural Netw. Learn. Syst.*, **35** (2024), 8702–8707. https://doi.org/10.1109/TNNLS.2022.3224065
41. X. Shi, C. C. Lim, P. Shi, S. Xu, Adaptive neural dynamic surface control for nonstrict-feedback systems with output dead zone, *IEEE Trans. Neural Netw. Learn. Syst.*, **29** (2018), 5200–5213. https://doi.org/10.1109/TNNLS.2018.2793968

AIMS Press

© 2024 the Author(s), licensee AIMS Press. This is an open access article distributed under the terms of the Creative Commons Attribution License (http://creativecommons.org/licenses/by/4.0)